Numerical modeling of digital devices impact on EMC/EMI

Numerical Modeling of Digital Devices Impact on EMC/EMI

F. Canavero, S. Grivet-Talocia, I. Maio, I. Stievano
Dip. Elettronica, Politecnico di Torino
Corso Duca degli Abruzzi 24
I-10129, Torino, Italy

Abstract: One of the most important issues for the assessment of EMI/EMC of modern electronic systems is the characterization of fast switching digital devices. Their nonlinear behavior strongly affects the integrity of signals launched on system interconnects, which in turn affect crosstalk and radiation. The system-level EMC is therefore highly sensitive to the nonlinear behavior of individual IC ports, which must be accounted for in any realistic numerical model. This paper considers several simplified approaches for modeling digital IC ports, with the aim of detecting which are the most important effects that must be considered for both signal integrity and radiated emission analyses.

1 INTRODUCTION

This paper deals with the characterization of digital IC ports, hereafter denoted generically as *drivers,* for EMC modeling. It is well known that drivers usually exhibit strong nonlinear dynamic behavior, that is best reproduced by detailed transistor-level models. However, such models are either not available or too complex for signal integrity and radiation analyses. Equivalent models have to be devised on the basis of possibly limited available informations, with the twofold objective of being simple and accurate at the same time. Of course, a trade-off between these two contrasting requirements must be sought for. In the following sections we will attempt a quantitative analysis, with the aim of pointing out which are the relevant effects that must be considered in order to guarantee sufficient accuracy for EMC purposes, and conversely which are the effects that may be neglected for the construction of simple driver models.

The outline of this paper is as follows. Section 2 presents a set of simplified models for the characterization of the switching driver behavior. Then, the accuracy of the proposed models is tested through significative benckmarks for signal integrity/crosstalk (section 3) and radiation (section 4) predictions. Finally, conclusions are drawn in section 5.

2 MODELS FOR DIGITAL DEVICES

This section reviews several linear and nonlinear simplified models for a specific driver, namely a 4-stage 1.2μm low-voltage CMOS driver. The methodology for constructing such models is however general (it applies in principle to any driver) and well known. The rationale for using any of the proposed models will also be given.

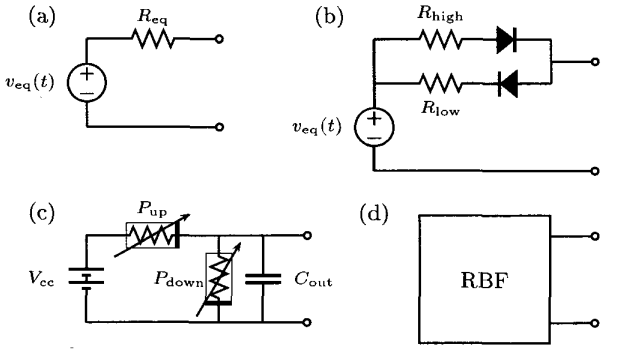

Figure 1: Equivalent circuits of various simplified driver models.

Due to the nonlinear behavior of the driver output characteristic, the switching waveforms for output voltage and current are highly dependent on the driven load. Moreover, the data usually available to the PCB designer about transient waveforms are commonly referred to a typical and specific load. It is guaranteed that the behavior of the device will be correctly reproduced only when such load is connected to the driver. When the load is changed, significantly different waveforms might be obtained. In the following we will consider the aforementioned device loaded with a $R_{ref} = 100\,\Omega$ resistor, since we intend to drive a transmission line with the same characteristic impedance. We will record the transient waveform under this load condition and we will construct the simplified models trying to approximate such switching behavior.

The considered models are listed below. In order to distinguish between different models we adopt a special rule for their denomination. All the results that will be presented will refer to this naming convention.

Model `M0`. This is a linear model consisting of a series Thevenin equivalent circuit (Fig. 1a). It is the simplest model that can be used to represent the driver switching behavior. The internal resistance is computed as the average between the two output (linear) resistances seen in the high and low port states, i.e., $R_{eq} = 0.5(R_{high} + R_{low})$. A rough approximation for the latter can be easily derived from technical datasheets. The equivalent voltage source $v_{eq}(t)$ is determined as an approximation of the transient switching waveform under reference

0-7803-6569-0/01/$10.00 © 2001 IEEE

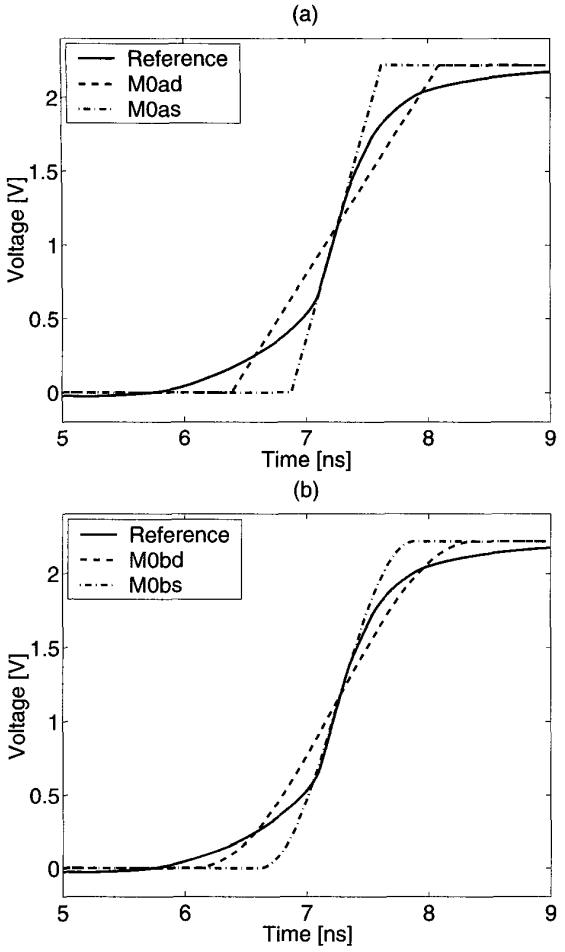

Figure 2: Construction of equivalent linear models from the transient switching waveform of the transistor-level driver model computed with a reference load $R_{\text{ref}} = 100\Omega$.

load conditions. Also in this case informations from technical datasheets can be used, like e.g. rise/fall times. Several possibilities for constructing the $v_{\text{eq}}(t)$ waveform are available.

`M0a` An equivalent trapezoidal waveform is determined with appropriate start and rise/fall times (Fig. 2a).

`M0b` A smooth waveform is determined through a raised-cosine function with appropriate start and rise/fall times (Fig. 2b). This second strategy should allow for better representations of the waveform.

For both trapezoidal (`'a'`) and raised cosine (`'b'`) waveforms the slope (directly related to the rise/fall time) can be determined in two ways. Each possibility is coded by an additional suffix that is appended to the model name.

`'d'` The slope is constructed in order to get the same rise time of the reference waveform between its 10% and 90% levels.

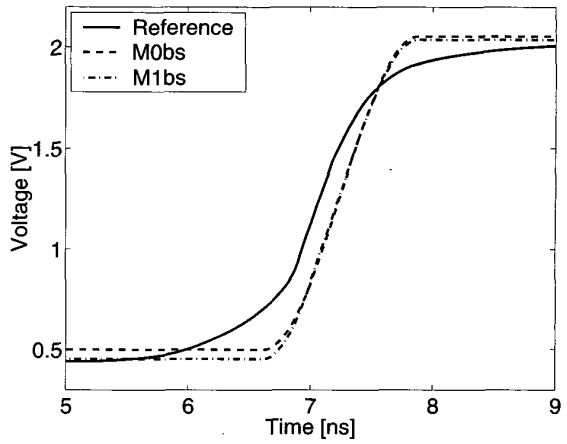

Figure 3: Sensitivity of linear/piecewise linear driver models under variable load (here a series of a 40Ω resistor and 1V battery).

`'s'` The approximate and reference curves are tangent at the 50% levels. Of course, this procedure can only be applied if either the complete switching waveform or the detailed `TL` model is available.

From Fig. 2 it can be seen that the start times are selected for all models in order to get synchronization at the 50% level. This is important for accurate signal integrity and timing analyses. We remark that the particular choice the above-listed models depends on the approximation rules that the designer intends to use, which is somewhat arbitrary and is not dictated by some *a priori* guideline except simplicity.

Model `M1`. This is a piecewise linear model which differs from model `M0` only through the series resistance. Two different values are used when the driver is in the high or low state, leading to the equivalent circuit of Fig. 1b. The equivalent voltage source $v_{\text{eq}}(t)$ is constructed accordingly to the rules listed for model `M0`. No plots are reported for this case since they match perfectly those of model `M0` when the driver is connected to the reference load. However, when the driver load is changed, model `M1` allows for better approximation of the steady states with respect to model `M0`. This is depicted in Fig. 3, where the performance of models `M0bs` and `M1bs` are compared to the response of the transistor-level model, when the load is a series connection of a 40 Ω resistor and a 1V constant voltage source. We can notice that both models fail in the approximation of the correct timing (always measured at the 50% level). This plot confirms that use of models `M0` and `M1` (i.e., linear or piecewise linear) may lead to wrong results in a signal integrity and timing analysis. If necessary, an output capacitance can also be connected in parallel to the output port of the driver model. We did verify that in the present case addition of the output capacitance does not lead to significantly improved results.

Model `N`. This model includes both the nonlinear and the dynamic behavior of the driver. Actually, there are several different approaches for the definition and generation of such

equivalents. These can be subdivided into two main classes

- `Nx` Such models are constructed by guessing a particular structure of a nonlinear and dynamic equivalent circuit, and subsequently characterizing each element by an estimation procedure [5]. Models based on the Input/output buffer Information Specification (IBIS), which have become *de facto* an industry standard, belong to this class. An example is given in Fig. 1c, where two nonlinear resistors with suitable characteristics represent the pull-up and pull-down parts of the driver.
- `Ny` These are behavioral models constructed in order to represent the port nonlinear dynamic behavior as a mathematical model. Models based on Radial Basis Functions (RBF) approximations [1] belong to this class. The latter are characterized by rigorous mathematical foundations, efficient estimation algorithms, and high insensitivity to the loads connected to the driver. A sketch of such models can be found in Fig. 1d.

No plots on the behavior of such nonlinear/dynamic models are reported here since the transient waveforms are undistinguishable from those relative to the transistor-level of the present driver. Models of class `Nx` or `Ny` must be used when very accurate analyses are to be performed. This will be illustrated by the numerical experiments in the next sections.

It can be desumed that the various models have been introduced here in ascending order of complexity or, equivalently, of accuracy. In the following sections we will try to identify which of such simplified models can be used for specific EMC analyses, by performing several benchmarks on actual drivers.

3 SIGNAL INTEGRITY AND CROSSTALK

In this section we test the performance of various simplified driver models for signal integrity and crosstalk analysis. We will consider the three-conductor (plus reference) lossy transmission line depicted in Fig. 4. Details on this structure can be found in [4]. Three identical drivers are connected on the near-end side, of which two are kept in a quiet (low) state and one is switching from low to high state. Three identical 1pF capacitors in parallel with 1kΩ resistors constitute the far-end loads. We will compute termination voltages and currents both on the active line and on victim lines.

The driver that we employ throughout this section is a commercial low-voltage CMOS driver, namely the `74LVC244`. For this device a detailed nominal transistor-level model is available, as well as IBIS data for a construction of a nonlinear dynamic simplyfied model of type `Nx`. It is well known that all the parameters in IBIS are available in typical, minimum, and maximum values. In order to test the sensitivity of the results on the various parameters we constructed a typical model (with label `Nxtyp`), a slow model including the smallest output currents together with the largest parasitic elements (label `Nxslow`), and a fast model with the largest output currents and the smallest parasitic elements (label `Nxfast`). We remark that these models are constructed from data made publicly available from the vendor, and not from direct measurements performed on the actual `TL` model. Finally, starting from the `TL` model, we

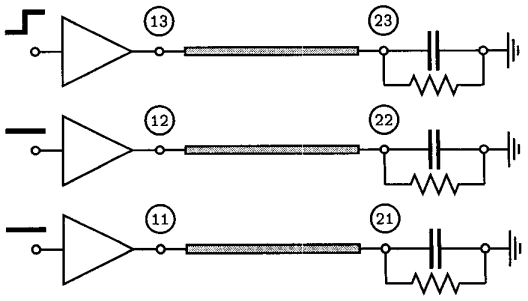

Figure 4: Coupled-line structure for the comparison of various driver models. Far-end loads are made of equal resistors (1kΩ) and capacitors (1pF).

constructed a behavioral RBF model of the type `Ny`. All these models are implemented as SPICE subcircuits in order to compare their responses within the same simulation environment.

The top panel in Fig. 5 shows the far-end crosstalk voltage $v_{22}(t)$. We note that the response of model `Ny` is undistinguishable from the reference `TL` curve. Model `M1bs` overestimates in this case crosstalk (but we will see in next section that it may underestimate radiated fields). We verified that the accuracy of other `M0` and `M1` models is at most comparable to that of model `M1bs`, so we do not report additional curves in the plots to avoid confusion. Model `Nxtyp` (but the same applies to the `slow` and `fast` implementations) underestimates crosstalk, and therefore its performance is comparable to that of equivalent linear/piecewise linear models. This shows that potentially accurate nonlinear models may be comparable to much simpler linear models due to the degraded precision at which they are made publicly available.

The bottom panel of Fig. 5 reports voltage $v_{13}(t)$. Again, the `Ny` (not shown) and the reference model give undistinguishable responses. We remark that all `Nx` models exploit a slower rise time than the reference. Threfore, even when variations in the parameters are considered, poor predictions may arise. In constrast, the piecewise linear model `M1bs` gives acceptable results, except for the fine details of the switching front.

4 RADIATION

This section briefly describes the precedure that is employed to calculate radiated fields from transmission-line structures terminated by any of the above listed devices models. Although the main interest here is on PCB structures loaded with several components and with high interconnect density, we will adopt several simplifying assumptions, detailed in the following paragraphs. These are justified by the specific target of the paper, which is to investigate the effect of nonlinearities of devices models on EMC prediction.

The computation of radiated fields from a given structure including possibly complex nonlinear devices is a challenging task, since inclusion of realistic components models into full-wave solvers does not appear to be feasible in a simple way. Therefore, in order to avoid complex nonlinear full-wave simulations, we split the radiation prediction into two separate steps. First,

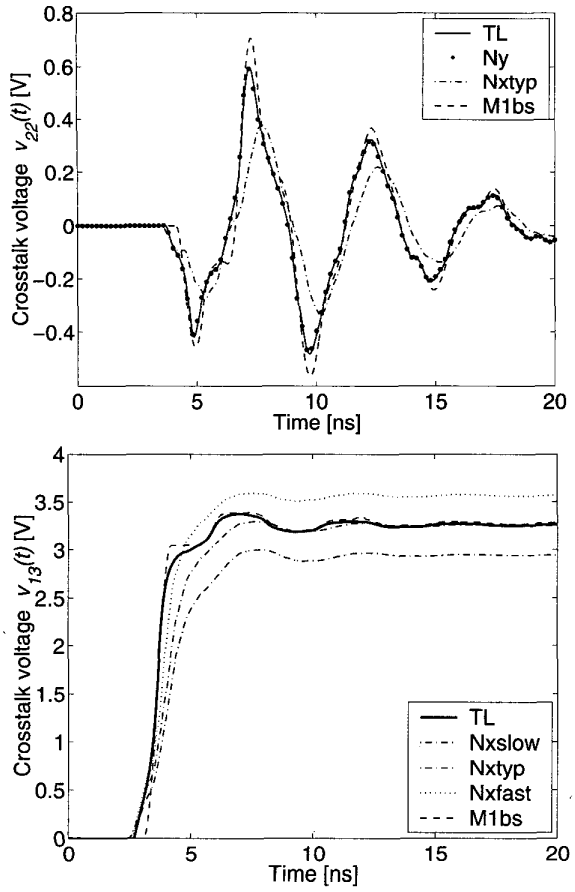

Figure 5: Signal integrity analysis of structure in Fig. 4 using different driver models. Voltage $v_{22}(t)$ (top panel) and $v_{13}(t)$ (bottom panel).

the current distributions in the system conductors are computed through circuit simulations including only propagation effects along transmission lines. Second, these currents are used to predict radiated fields through spatial convolutions with appropriate Green's functions. Indeed, once the currents are completely known, the radiation prediction can be performed directly in the frequency domain since the link between currents and fields is linear and superposition applies.

The main differences between the performance of various linear/nonlinear models of the devices arise in the first step of the simulation process. It is clear that different models will indeed lead to quite different current distributions along the system conductors. However, once the currents are computed, the procedure for the computation of radiated fields does not differ for the various termination models, since the currents are the starting point of the radiation prediction. This is true both if we consider a real PCB structure with dielectric substrate and complex ground plane geometries, or a simplified geometry with no ground planes and the dielectric removed. In the first case, the computation of the fields may result quite complex, while in the second case the free space Green's function may be applied. Therefore, the presence of complex geometries only complicates the mathematical formulation of the radiation prediction and the computations, without significantly affecting the difference between the performances of the various termination models. For this reason we propose to use a drastically simplified benchmark structure, namely conductors in free space, in order to deal with the radiation part in the most simple way, nonetheless retaining all the significant differences between the linear/nonlinear models in the computed fields.

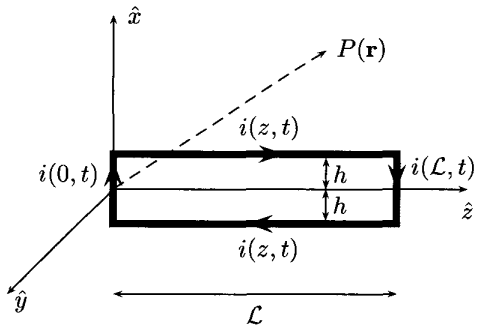

Figure 6: Structure adopted for the computation of radiated electric field at a given location $P(\mathbf{r})$

The structure that will be investigated, depicted in Fig. 6, is a two-conductor transmission line with small cross section. The two conductors carry the same current $i(z,t)$ flowing in opposite direction, therefore only differential-mode currents are dealt with in this paper. The driver and receiver are modeled with vertical risers connecting the two conductors at their edges. These two segments carry the currents $i(0,t)$ and $i(\mathcal{L},t)$, respectively, in order to insure continuity of the loop currents. These risers have significant effect in the radiated field since their current may be quite different if the line is electrically long.

The simulations performed in this work to compute the current distributions follow a two-step procedure, depicted in Fig. 7. Since all models for terminations have been coded as SPICE equivalent circuits, we use SPICE for computing first the termination voltages and currents of a specific terminated transmission line. At this stage it is also possible to adopt complete transistor-level models for the drivers/receivers. The procedure for the generation of an appropriate SPICE model for the line with an arbitrary number of conductors, and possibly frequency-dependent losses, is taken from [4]. The results of SPICE return only the termination voltages $v(0,t)$, $v(\mathcal{L},t)$ and currents $i(0,t)$, $i(\mathcal{L},t)$, but not the overall current distribution along the conductors, which is needed for radiation predictions. We resort then to the substitution theorem [2] and we replace the complex line terminations with frequency-domain equivalent voltage sources $V_0^{\text{eq}}(\omega) = \mathcal{F}\{v(0,t)\}$ and $V_{\mathcal{L}}^{\text{eq}}(\omega) = \mathcal{F}\{v(\mathcal{L},t)\}$. The resulting structure can be solved for the current distribution $I(z,\omega)$ through standard transmission-line theory [6] or through some finite-difference scheme as in [3].

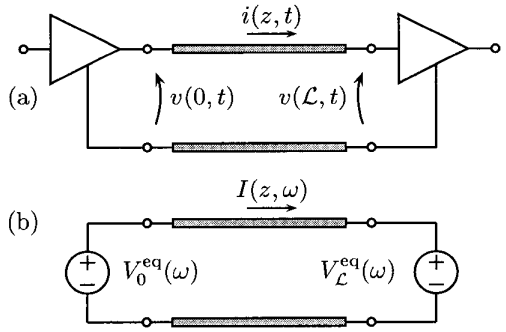

Figure 7: Application of the substitution theorem for the computation of the current distribution. First (a) the termination voltages $v(0,t)$, $v(\mathcal{L},t)$ are computed through a SPICE simulation including possibly nonlinear models for drivers/receivers. Then (b) the frequency-domain current distribution $I(z,\omega) = \mathcal{F}\{i(z,t)\}$ is computed solving an equivalent linear structure with the terminations replaced by voltage sources $V_0^{\rm eq}(\omega) = \mathcal{F}\{v(0,t)\}$ and $V_{\mathcal{L}}^{\rm eq}(\omega) = \mathcal{F}\{v(\mathcal{L},t)\}$.

The overall structure of Fig. 6 is placed in free space. Therefore, we proceed in using the free-space dyadic Green's function to compute radiated fields. In the following, we report the well known expressions leading to the computed electric field at any desired point $P(\mathbf{r})$, denoting with boldface vector or dyadic quantities. The free-space dyadic Green's function reads

$$\mathbf{G}(\mathbf{r}) = \left[\mathbf{I} + \frac{\nabla\nabla}{k_0^2}\right]\varphi(r),$$

where $k_0 = \omega\sqrt{\varepsilon\mu}$, $\mathbf{I}$ is the unitary dyadic operator and

$$\varphi(r) = \frac{1}{4\pi r}e^{-jk_0 r}.$$

The expression of the radiated electric field from a current density $\mathbf{J}_e(\mathbf{r}')$ is

$$\mathbf{E}(\mathbf{r}) = -j\omega\mu\int \mathbf{G}(\mathbf{r}-\mathbf{r}')\cdot\mathbf{J}_e(\mathbf{r}')\,\mathrm{d}\mathbf{r}'.$$

In the structure under investigation the current density can be approximated as a superposition of elementary Hertzian dipoles at location $\mathbf{r}_n$

$$\mathbf{J}_e(\mathbf{r}') = \sum_n \mathbf{M}_n\,\delta(\mathbf{r}'-\mathbf{r}_n).$$

with dipole moments $\mathbf{M}_n$ directly related to the frequency-domain current distribution

$$\mathbf{M}_n = \widehat{I}_n(s,\omega)\,\Delta s\,\hat{\mathbf{s}},$$

where $\widehat{I}_n(s,\omega)$ is the (constant) current flowing along the n-th segment of size Δs with orientation $\hat{\mathbf{s}}$. The number of dipoles employed in the discretization of the line conductors is determined from the electrical length of the line at the highest frequency of interest, while only one equivalent dipole is used for the vertical risers. In summary, the radiated electric field reads

$$\mathbf{E}(\mathbf{r}) = -j\omega\mu\sum_n \mathbf{G}(\mathbf{r}-\mathbf{r}_n)\cdot\mathbf{M}_n$$

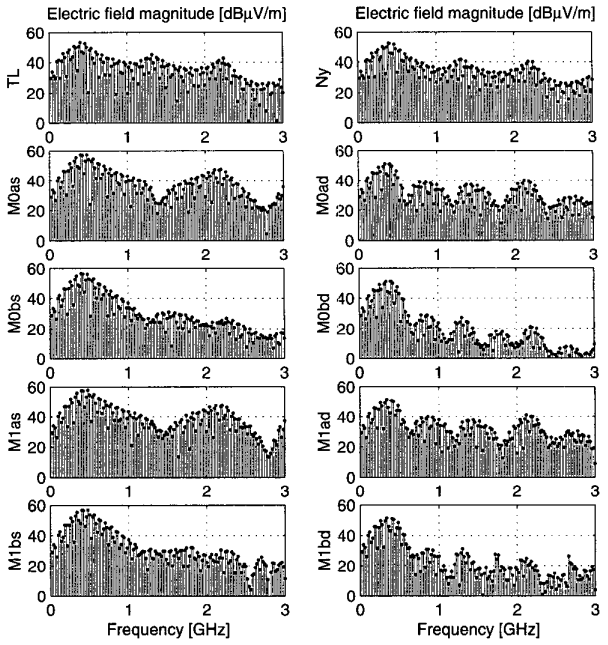

Figure 8: Magnitude of radiated electric field at a distance of 3m from the structure for different driver models.

The first numerical experiment illustrates that simplified linear models may lead to quite erroneous results for predicted radiated fields. The structure under investigation is depicted in Fig. 6. The line length is $\mathcal{L} = 15$cm, with a separation between the conductors of $2h = 5$mm. The line characteristic impedance is $Z_\infty = 100\Omega$, the left termination is the 4-stage CMOS driver already used in Sec. 2, while the right termination is a 1pF capacitor. Figure 8 shows the radiated electric field at a distance $d = 3$m from the structure (and equal angular deviation from the three axes) obtained replacing the driver with one of the simplified models under investigation (we remark that similar results were obtained for different directions). We report results up to a frequency of 3GHz since future trends in EMC regulations will inevitably lead to extensions into higher frequencies of the current emission limits. The top left figure is the reference curve, obtained with the fully detailed `TL` model of the driver. The top right panel illustrates the performance of a RBF-based nonlinear dynamic driver model. The results are almost undistinguishable from the reference emission profile. Conversely, the bottom panels (all related to linear/piecewise linear models) fail at some frequencies to predict the correct emissions. In particular, the models `M0bd`, `M1bd`, based on smooth raised-cosine waveforms with matched rise times (that would be expected to represent fairly well the driver switching behavior) fail completely the prediction for frequencies higher than about 500MHz. In addition, the behavior of linear `M0` and piecewise linear `M1` models is almost the same, since more accurate representation of steady-state levels has almost no influence on the high frequency spectral components. This figure allows to conclude that linear/piecewise linear models should not be used for radiation prediction, and that fully nonlinear models are

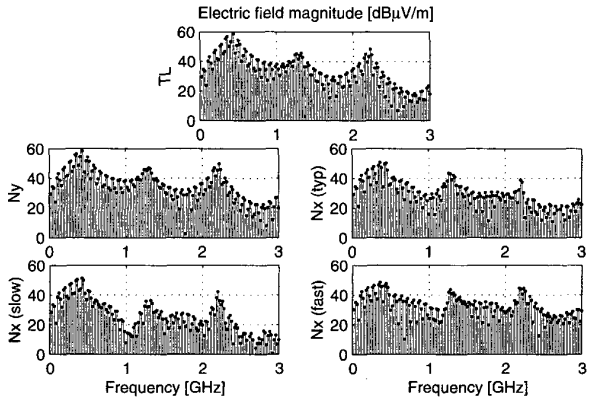

Figure 9: Magnitude of radiated electric field at a distance of 3m from the structure for different nonlinear dynamic models of driver 74LVC244.

necessary not only for signal integrity simulations but also for radiated emissions modeling.

The second numerical experiment refers to the same structure excited by a different driver. We use here the 74LVC244 CMOS driver already employed in the signal integrity analyses of the foregoing section. In particular, we compare the accuracy of various nonlinear dynamic models (Nx, Ny) looking at the radiated electric field. We remark again that we know the transistor-level model of the device, which allows us to derive reference emission profiles. The right line termination is made of a 1pF capacitor in parallel with a 1kΩ resistor. Figure 9 reports the simulation results. The top panel is the reference emission profile obtained with the full transistor-level driver model. The left panel in second row is the outcome of RBF-based model Ny. It almost matches the reference radiated field. The three remaining panels refer to different implementations of Nx models based on IBIS data set, namely the typical, slow and fast models. These clearly underestimate the radiated electric field by a considerable amount throughout the investigated frequency band. The reason for this discrepancies may be identified with the reduced accuracy at which IBIS data are usually made available.

5 CONCLUSIONS

Several different approaches for modeling the transient behavior of digital devices for EMC purposes can be followed. We detailed in this paper some linear, piecewise linear, or fully nonlinear dynamic models. The numerical experiments that we performed on typical drivers show that linear and piecewise linear models allow for accuracies that may not be sufficient for signal integrity, crosstalk, and radiated emissions analyses. The models that we found to be very accurate for all types of simulations are nonlinear dynamic models like, e.g., those based on Radial Basis Functions (RBF). We showed that nonlinear dynamic models derived from public IBIS datasets may be quite inaccurate for EMC purposes due to the degraded precision at which they are commonly available to designers and end-users.

REFERENCES

[1] F. G. Canavero, I. A. Maio, I. S. Stievano, "Black-Box Models of Digital IC ports for EMC simulations," in *14th IEEE International Zurich Symposium on Electromagnetic Compatibility,* Zurich, CH, pp. 679–684, February 20–22, 2001.

[2] L. O. Chua, C. A. Desoer, E. S. Kuh, *Linear and Nonlinear Circuits,* McGraw-Hill, NY, 1987.

[3] S. Grivet-Talocia and F. Canavero, "Weak boundary treatment for high order transient analysis of MTL's," in *IEEE International Symposium on Electromagnetic Compatibility, Washington, DC,* pp. 409–414, August 21-25, 2000.

[4] I. A. Maio, F. G. Canavero, B. Dilecce, "Analysis of crosstalk and field coupling to lossy MTL's in a SPICE environment", IEEE Trans. on EMC, Vol. 38, No. 3, August 1996.

[5] I. A. Maio, I. S. Stievano, F. G. Canavero, "Signal Integrity and Behavioral Models of Digital Devices," in *13th International Zurich Symposium on Electromagnetic Compatibility,* Zurich, CH, pp. 149–154, February 13–15, 1999.

[6] C. R. Paul, *Analysis of Multiconductor Transmission Lines,* John Wiley and Sons, NY, 1994.